protection against ROS could be important for cellular survival. In addition, mitochondrial dysfunction induces apoptosis by releasing cytochrome C to the cytoplasm [40,44,45]. Therefore, mitochondrial protection could be important to protect cells against apoptosis. Our results, in conjunction with reported similar improvements by the mitochondrial LEA protein of Artemia [18], suggest that the preservation of mitochondrial integrity is important and partly sufficient to afford cellular tolerability against water stress. Simultaneous introduction of molecules that protect other cellular compartments could further enhance tolerability.

In our previous heat-soluble proteome analysis, we identified two tardigrade-unique heat-soluble protein families, CAHS and SAHS, as predominant heat-soluble proteins in the anhydrobiotic tardigrade *R. varieornatus*. Neither MAHS nor RvLEAM was detected in the previous study, possibly due to the small proportion of mitochondria in the tardigrade lysate, and thus other proteins in the cytoplasm and/or extracellular space might overwhelm MAHS and RvLEAM. To date, three tardigrade-unique heat-soluble protein families have been identified, MAHS, CAHS, and SAHS. Their subcellular localizations are mutually exclusive and together they cover most cellular components: MAHS in the mitochondria, CAHS in the cytoplasm and nucleus, and SAHS in the extracellular space and secretory organelles.

These tardigrade-unique heat-soluble proteins are hydrophilic and have biochemical properties similar to LEA proteins, suggesting their involvement in tolerability, but experimental evidence was lacking. The present study provides the first evidence that newly identified MAHS, a tardigrade-unique heat-soluble protein, confers tolerability against water stress. This is the first report of the protective effect of tardigrade-unique heat-soluble proteins.

Why have tardigrades evolved to utilize such unique heat-soluble protein complements alongside LEA proteins, unlike other anhydrobiotic animals? The difference in trehalose accumulation might be a clue to answering this question. Anhydrobiotic arthropods and nematodes in a dehydrated state accumulate large amounts of trehalose [4–6]. In contrast, there is no or low accumulation of trehalose in anhydrobiotic tardigrades [8], thus an alternative protective mechanism/molecule might be required. Tardigrade-unique heat-soluble proteins, including MAHS identified in this study, are candidate protective proteins that complement the small amount of trehalose present.

We identified the first mitochondrial complement of tardigrade-unique heat-soluble proteins and demonstrated its protective activity. The current repertoire of tardigrade-unique heat-soluble proteins covers various cellular components, including mitochondria, which seem to be key target organelles to confer protection to cells against water stress. This repertoire of proteins provides clues to help elucidate the protection mechanism of tardigrades against stress, and may contribute to the development of a method to confer more robust tolerability to stress-sensitive cells of other species, including humans.

Supporting Information

S1 Fig. Multiple alignments of LEAM proteins among tardigrade species.
(TIF)

S2 Fig. Specific reactivity of anti-RvLEAM antiserum and anti-ATP5A antibody in immunohistochemistry.
(TIF)

S3 Fig. Characteristics of predicted tardigrade-unique proteins in mitochondria.
(TIF)

S4 Fig. Multiple alignments of MAHS proteins among tardigrade species.
(TIF)

S1 Table. Subcellular localization of potential mitochondria-targeted LEA protein and tardigrade-unique proteins.
(TIF)

Author Contributions

Conceived and designed the experiments: ST T. Kubo T. Kunieda. Performed the experiments: ST. Analyzed the data: ST T. Kunieda. Contributed reagents/materials/analysis tools: JT YM DH T. Katayama KA AT. Wrote the paper: ST T. Kubo T. Kunieda.

References

1. Møbjerg N, Halberg KA, Jørgensen A, Persson D, Bjørn M, Ramløv H, et al. (2011) Survival in extreme environments—on the current knowledge of adaptations in tardigrades. Acta physiologica (Oxford, England) 202: 1748–1716.
2. Jönsson KI, Rabbow E, Schill RO, Harms-Ringdahl M, Rettberg P. (2008) Tardigrades survive exposure to space in low Earth orbit. Curr. Biol. 18: R729–R731. doi: 10.1016/j.cub.2008.06.048 PMID: 18786368
3. Persson D, Halberg K A, Jørgensen A, Ricci C, Møbjerg N, Kristensen RM. (2011) Extreme stress tolerance in tardigrades: surviving space conditions in low earth orbit. J. Zoolog. Syst. Evol. Res. 49: 90–97.
4. Clegg JS. (1965) The origin of trehalose and its significance during emergence ofencysted dormant embryos of Artemia salina. Comp. Biochem. Physiol. 14: 135–143. PMID: 14288194
5. Madin KAC, Crowe JH. (1975) Anhydrobiosis in nematodes: carbohydrate and lipid metabolism during dehydration. J. Exp. Zool. 193: 335–342,
6. Watanabe M, Kikawada T, Okuda T. (2003) Increase of internal ion concentration triggers trehalose synthesis associated with cryptobiosis in larvae of Polypedilum vanderplanki. J. Exp. Biol. 206: 2281–2286. PMID: 12771176
7. Tunnacliffe A, Lapinski J, McGee B. (2005) A putative LEA protein, but no trehalose, is present in anhydrobiotic bdelloid rotifers. Hydrobiologia 546: 315–321.
8. Hengherr S, Heyer AG, Kohler H-R, Schill RO. (2008) Trehalose and anhydrobiosis in tardigrades-evidence for divergence in responses to dehydration. FEBS J. 275: 281–288. PMID: 18070104
9. Hand SC, Menze MA, Toner M, Boswell L, Moore D. (2011) LEA proteins during water stress: not just for plants anymore. Annu. Rev. Physiol. 73: 115–134. doi: 10.1146/annurev-physiol-012110-142203 PMID: 21034219
10. Browne JA, Dolan KM, Tyson T, Goyal K, Tunnacliffe A, Burnell AM. (2004) Dehydration-specific induction of hydrophilic protein genes in the anhydrobiotic nematode Aphelenchus avenae. Eukaryot. Cell. 3: 966–975. PMID: 15302829
11. Kikawada T, Nakahara Y, Kanamori Y, Iwata K, Watanabe M, McGee B, et al. (2006) Dehydration-induced expression of LEA proteins in an anhydrobiotic chironomid. Biochem. Biophys. Res. Commun. 348: 56–61. PMID: 16875677
12. Battaglia M, Olvera-Carrillo Y, Garciarrubio A, Campos F, Covarrubias AA. (2008) The enigmatic LEA proteins and other hydrophilins. Plant Physiol. 148: 6–24. doi: 10.1104/pp.108.120725 PMID: 18772351
13. Tunnacliffe A, Wise MJ. (2007) The continuing conundrum of the LEA proteins. Naturwissenschaften. 94: 791–812. PMID: 17479232
14. Goyal K, Walton LJ, Tunnacliffe A. (2005) LEA proteins prevent protein aggregation due to water stress. Biochem. J. 388: 151–157. PMID: 15631617
15. Pouchkina-Stantcheva NN, McGee BM, Boschetti C, Tolleter D, Chakrabortee S, Popova AV, et al. (2007) Functional divergence of former alleles in an ancient asexual invertebrate. Science 318: 268–271. PMID: 17932297
16. Chakrabortee S, Boschetti C, Walton LJ, Sarkar S, Rubinsztein DC, Tunnacliffe A. (2007) Hydrophilic protein associated with desiccation tolerance exhibits broad protein stabilization function. Proc. Natl. Acad. Sci. U. S. A. 104: 18073–18078. doi: 10.1073/pnas.0706964104 PMID: 17984052
17. Li S, Chakraborty N, Borcar A, Menze MA, Toner M, Hand SC. (2012) Late embryogenesis abundant proteins protect human hepatoma cells during acute desiccation. Proc. Natl. Acad. Sci. U.S.A. 18: 20859–20864.

18. Marunde MR, Samarajeewa DA, Anderson J, Li S, Hand SC, Menze MA. (2013) Improved tolerance to salt and water stress in Drosophila melanogaster cells conferred by late embryogenesis abundant protein. J. Insect Physiol. 59: 377–386. doi: 10.1016/j.jinsphys.2013.01.004 PMID: 23376561

19. Tripathi R, Boschetti C, McGee B, Tunnacliffe A. (2012) Trafficking of bdelloid rotifer late embryogenesis abundant proteins. J. Exp. Biol. 215: 2786–2794. doi: 10.1242/jeb.071647 PMID: 22837450

20. Förster F, Liang C, Shkumatov A, Beisser D, Engelmann JC, Schnölzer M, et al. (2009) Tardigrade workbench: comparing stress-related proteins, sequence-similar and functional protein clusters as well as RNA elements in tardigrades. BMC Genomics 10: 469. doi: 10.1186/1471-2164-10-469 PMID: 19821996

21. Mali B, Grohme MA, Förster F, Dandekar T, Schnölzer M, Reuter D, et al. (2010) Transcriptome survey of the anhydrobiotic tardigrade Milnesium tardigradum in comparison with Hypsibius dujardini and Richtersius coronifer. BMC Genomics 11: 168. doi: 10.1186/1471-2164-11-168 PMID: 20226016

22. Förster F, Beisser D, Grohme MA, Liang C, Mali B, Siegl AM, et al. (2012) Transcriptome analysis in tardigrade species reveals specific molecular pathways for stress adaptations. Bioinform. Biol. Insights 6: 69–96. doi: 10.4137/BBI.S9150 PMID: 22563243

23. Yamaguchi A, Tanaka S, Yamaguchi S, Kuwahara H, Takamura C, Imajoh-Ohmi S, et al. (2012) Two Novel Heat-Soluble Protein Families Abundantly Expressed in an Anhydrobiotic Tardigrade. PLoS ONE 7: e44209. doi: 10.1371/journal.pone.0044209 PMID: 22937162

24. Horikawa DD, Kunieda T, Abe W, Watanabe M, Nakahara Y, Yukuhiro F, et al. (2008) Establishment of a rearing system of the extremotolerant tardigrade Ramazzottius varieornatus: a new model animal for astrobiology. Astrobiology 8: 549–556. doi: 10.1089/ast.2007.0139 PMID: 18554084

25. Horton P, Park KJ, Obayashi T, Fujita N, Harada H, Adams-Collier CJ, et al. (2007) WoLF PSORT: protein localization predictor. Nucleic Acids Res. 35: W585–W587. PMID: 17517783

26. Emanuelsson O, Nielsen H, Brunak S, von Heijne G. (2000) Predicting subcellular localization of proteins based on their N-terminal amino acid sequence. J. Mol. Biol. 300: 1005–1016. PMID: 10891285

27. Nielsen H, Engelbrecht J, Brunak S, von Heijne G. (1997) Identification of prokaryotic and eukaryotic signal peptides and prediction of their cleavage sites. Protein Eng. 10: 1–6. PMID: 9239223

28. Claros MG, Vincens P. (1996) Computational method to predict mitochondrially imported proteins and their targeting sequences. Eur. J. Biochem. 241: 779–786. PMID: 8944766

29. Pollastri G, McLysaght A. (2005) Porter: a new, accurate server for protein secondary structure prediction. Bioinformatics 21: 1719–1720. PMID: 15585524

30. Kyte J, Doolittle RF. (1982) A simple method for displaying the hydropathic character of a protein. J. Mol. Biol. 157: 105–132. PMID: 7108955

31. Zdobnov EM, Apweiler R. (2001) InterProScan—an integration platform for the signature-recognition methods in InterPro. Bioinformatics 9: 847–848.

32. Bailey TL, Elkan C. (1994) Fitting a mixture model by expectation maximization to discover motifs in biopolymers. Proc.Int. Conf. Intell. Syst. Mol. Biol. 2: 28–36. PMID: 7584402

33. Tanaka J, Miwa Y, Miyoshi K, Ueno A, Inoue H. (1999) Construction of Epstein-Barr virus-based expression vector containing mini-oriP. Biochem. Biophys. Res. Commun. 264: 938–943. PMID: 10544034

34. Dure L III. (1993) A repeating 11-mer amino acid motif and plant desiccation. Plant J. 3: 363–369. PMID: 8220448

35. Hatanaka R, Hagiwara-Komoda Y, Furuki T, Kanamori Y, Fujita M, Cornette R, et al. (2013) An abundant LEA protein in the anhydrobiotic midge, PvLEA4, acts as a molecular shield by limiting growth of aggregating protein particles. Insect Biochem. Mol. Biol. 43: 1055–1067. doi: 10.1016/j.ibmb.2013.08.004 PMID: 23978448

36. Iturriaga G. (2008) The LEA proteins and trehalose loving couple: a step forward in anhydrobiotic engineering. Biochem. J. 410, e1–2. doi: 10.1042/BJ20071633 PMID: 18254727

37. Sharon MA, Kozarova A, Clegg JS, Vacratsis PO, Warner AH. (2009) Characterization of a group 1 late embryogenesis abundant protein in encysted embryos of the brine shrimp Artemia franciscana. Biochem. Cell Biol. 87, 415–430. doi: 10.1139/o09-001 PMID: 19370059

38. Furuki T, Shimizu T, Chakrabortee S, Yamakawa K, Hatanaka R, Takahashi T, et al. (2012) Effects of Group 3 LEA protein model peptides on desiccation-induced protein aggregation. Biochim. Biophys. Acta. 1824: 891–897. doi: 10.1016/j.bbapap.2012.04.013 PMID: 22579671

39. Furuki T, Sakurai M. (2014) Group 3 LEA protein model peptides protect liposomes during desiccation. Biochim. Biophys. Acta. 1838: 2757–2766. doi: 10.1016/j.bbamem.2014.07.009 PMID: 25037007

40. Kroemer G, Galluzzi L, Brenner C. (2007) Mitochondrial membrane permeabilization in cell death. Physiol. Rev. 87: 99–163. PMID: 17237344

41. Pereira Ede J, Panek AD, Eleutherio EC. (2003) Protection against oxidation during dehydration of yeast. Cell Stress Chaperones. 8: 120–124. PMID: 14627197

42. Contreras-Porcia L, Thomas D, Flores V, Correa JA. (2011) Tolerance to oxidative stress induced by desiccation in Porphyra columbina (Bangiales, Rhodophyta). J. Exp. Bot. 62:1815–1829. doi: 10.1093/jxb/erq364 PMID: 21196477

43. Cruz de Carvalho R, Catalá M, Marques da Silva J, Branquinho C, Barreno E. (2012) The impact of dehydration rate on the production and cellular location of reactive oxygen species in an aquatic moss. Ann. Bot. 110: 1007–1016. doi: 10.1093/aob/mcs180 PMID: 22875812

44. Kroemer G, Reed JC. (2000) Mitochondrial control of cell death. Nat. Med. 6: 513–519. PMID: 10802706

45. Danial NN, Korsmeyer SJ. (2004) Cell death: critical control points. Cell. 116: 205–219. PMID: 14744432

STEM CELLS®

EMBRYONIC STEM CELLS/INDUCED PLURIPOTENT STEM CELLS

Biosynthesis of Ribosomal Rna in Nucleoli Regulates Pluripotency and Differentiation Ability of Pluripotent Stem Cells

KANAKO WATANABE-SUSAKI[1,5], HITOMI TAKADA[1,5], KEI ENOMOTO[2,5], KYOKO MIWATA[1], HISAKO ISHIMINE[1], ATSUSHI INTOH[2], MANAMI OHTAKA[1], MAHITO NAKANISHI[1], HIROMU SUGINO[1], MAKOTO ASASHIMA[1,2,3], AND AKIRA KURISAKI[1,4]

[1]Research Center for Stem Cell Engineering, National Institute of Advanced Industrial Science and Technology (AIST), Tsukuba Central 4, 1-1-1, Higashi, Tsukuba, Ibaraki 305-8562, Japan ; [2]Department of Life Sciences (Biology), Graduate School of Arts and Sciences, The University of Tokyo, 3-8-1, Komaba, Meguro-ku, Tokyo 153-8902, Japan; [3]ICORP Organ Regeneration Project, Japan Science and Technology Agency (JST), 3-8-1 Komaba, Meguro-ku, Tokyo 153-8902, Japan

[4]Correspondence should be addressed to A.K. (Research Center for Stem Cell Engineering, National Institute of Advanced Industrial Science and Technology (AIST), Tsukuba Central 4, 1-1-1, Higashi, Tsukuba, Ibaraki 305-8562, Japan. TEL: +81-29-861-2569, FAX: +81-29-861-2987, e-mail: akikuri@hotmail.com); [5]These authors equally contributed to this work.; Funding: This work was supported by JST PRESTO and Grant-in-Aid for Scientific Research (17510165 and 20610008). The funders had no role in study design, data collection and analysis, decision to publish, or preparation of the manuscript.

Received September 24, 2013; accepted for publication July 23, 2014

1066-5099/2014/$30.00/0

This article has been accepted for publication and undergone full peer review but has not been through the copyediting, typesetting, pagination and proofreading process which may lead to differences between this version and the Version of Record. Please cite this article as doi: 10.1002/stem.1825

Key Words. Fibrillarin • rRNA • ES cells • pluripotency • nucleoli • differentiation.

ABSTRACT

Pluripotent stem cells have been shown to have unique nuclear properties, e.g., hyperdynamic chromatin and large, condensed nucleoli. However, the contribution of the latter unique nucleolar character to pluripotency has not been well understood. Here, we show that fibrillarin (FBL), a critical methyltransferase for ribosomal RNA (rRNA) processing in nucleoli, is one of the proteins highly expressed in pluripotent embryonic stem (ES) cells. Stable expression of FBL in ES cells prolonged the pluripotent state of mouse ES cells cultured in the absence of leukemia inhibitory factor (LIF). Analyses using deletion mutants and a point mutant revealed that the methyltransferase activity of FBL regulates stem cell pluripotency. Knockdown of this gene led to significant delays in rRNA processing, growth inhibition, and apoptosis in mouse ES cells. Interestingly, both partial knockdown of FBL and treatment with actinomycin D, an inhibitor of rRNA synthesis, induced the expression of differentiation markers in the presence of LIF and promoted stem cell differentiation into neuronal lineages. Moreover, we identified p53 signaling as the regulatory pathway for pluripotency and differentiation of ES cells. These results suggest that proper activity of rRNA production in nucleoli is a novel factor for the regulation of pluripotency and differentiation ability of ES cells. STEM CELLS *2014; 00:000–000*

INTRODUCTION

Embryonic stem (ES) cells can undergo self-renewal while retaining the ability to differentiate into all types of cells in the body. Pluripotency of stem cells is regulated by a specific transcription network composed of core transcription factors such as Oct4, Sox2, and Nanog [1, 2]. On the other hand, ES cells have unique nuclear properties such as hyperdynamic chromatin and an unusual morphology of subnuclear compartments, including large nucleoli [3, 4]. In ES cells, the nucleoli undergo dynamic morphological changes during the differentiation process.

Nucleoli are the sites of ribosome biogenesis, ribosomal DNA transcription, pre-ribosomal RNA (rRNA) processing, and assembly of mature rRNAs with ribosomal proteins [5]. Nucleoli also have several roles in cellular processes, including cell-cycle control, regulation of mitosis, biogenesis of multiple ribonucleoproteins, and cellular stress responses [6]. The nucleolar size varies among cells and is dependent mainly on the activity of the organelle: fully active nucleoli are larger, whereas inactive nucleoli tend to be small and fragmented [7]. The size of nucleoli increases in growing cells in proportion to the amount of rRNA synthesized [8, 9]. Although a correlation between the pluripotency of ES cells and the characteristic morphology of nucleoli has been suggested, the direct contribution of nucleoli to pluripotency and differentiation ability of ES cells has not been explored.

Fibrillarin (FBL) is a specific marker for the dense fibrillar component, and indispensable for ribosome biogenesis. FBL functions as a catalytic center of C/D box small nucleolar ribonucleoprotein complexes that catalyze the 2′-*O*-methylation of rRNA [10-12]. In yeast, FBL is essential for cell viability [10, 12]. In mice, loss of the methyltransferase domain of FBL by gene targeting led to embryonic lethality before the blastocyst stage [13]. Previously, we performed proteomic analyses of mouse ES cells and identified FBL as one of the highly expressed proteins in pluripotent mouse ES cells [14].

In this study, we investigated the functions of nucleoli in pluripotent ES cells by modulating this principal nucleolar methyltransferase, FBL. We show that biosynthesis of rRNA regulates the maintenance and differentiation of ES cells through the p53 signaling pathway.

MATERIALS AND METHODS

Cell culture

The mouse ES cell line D3 was purchased from the American Type Culture Collection (ATCC, Manassas, VA). EBRTcH3, a mouse ES cell line used for knock-in experiments, was a kind gift from Drs. Hitoshi Niwa and Shinji Masui (Riken, Japan). These cells were maintained on feeder layers of mitomycin C-treated MEFs or 0.1% gelatin-coated dishes in ES medium, DMEM (high-glucose; Wako, Osaka, Japan) containing 15% heat-inactivated fetal calf serum (FCS, Roche, Mannheim, Germany), nonessential amino acids (Sigma-Aldrich, St. Louis, MO), 0.1 mM β-mercaptoethanol (Sigma-Aldrich), 0.1 mg/mL penicillin/streptomycin (Wako), and 1000 U/mL LIF (ESGRO; Chemicon, Billerica, MA). To prepare RNA and protein samples from pluripotent and differentiated cells, mouse ES cells were cultured for 10 days in the above medium in the presence or absence of LIF, respectively.

Plat-E packaging cells were kindly provided by Dr. Kitamura (University of Tokyo, Japan) [15] and were used to produce retroviruses. Plat-E cells were maintained in DMEM (low-glucose; Wako) containing 10% FCS, 0.1 mg/mL penicillin/streptomycin, 1 μg/mL puromycin (Sigma-Aldrich), and 10 μg/mL blasticidin (Life Technologies). The human cell lines HeLa and HaCaT and the mouse cell lines C2C12 and KUM9 were maintained in DMEM (low-glucose; Wako) containing 10% FCS and 0.1 mg/mL penicillin/streptomycin (Wako). KUM9 cells were generously provided by Dr. Umezawa (NCCHD, Japan).

Plasmid construction

Full-length and deletion mutants of FBL expression plasmids were constructed with a PCR-amplified DNA fragment using plasmids encoding full-length FBL (pcDNA3.1[+]-FBL) and the deletion mutants (pcDNA3.1[+]-FIB IV for FBL-N and FIB III for FBL-C) [16] as templates. The PCR primer sets were as follows: for full-length FBL, forward, 5′-GGA ATT CGC CAC CAT GGA CTA CAA GGA C-3′ and reverse, 5′-GCT CTC GAG TCA GTT CTT CAC CTT GGG GGG-3′; for the deletion mutants of FBL, forward for both FBL-N and FBL-C, 5′-GGA ATT CGC CAC CAT GGA CTA CAA GGA C-3′ and reverse for FBL-N, 5′-CTC GCG GCC GCT CAT CGG TAC TCA ATT TTG TCA TC-3′, and reverse FBL-C, 5′-CTC GCG GCC GCT CAG TTC TTC ACC TTG GGG G-3′. The full length cDNA were amplified with a high-fidelity PCR enzyme, KOD-Plus (TOYOBO, Osaka, Japan), digested with *EcoR*I and *Xho*I, and inserted between the *EcoR*I and *Xho*I sites of the pCAG-IP vector [17]. Similarly, the deletion mutant cDNAs were amplified and inserted between *EcoR*I and *Not*I sites of the same vector. All constructed pCAG-IP-based expression vectors for the generation of FBL proteins were FLAG-tagged at the N-terminus.

Point mutations in FBL were introduced by PCR-based site-directed mutagenesis using KOD-Plus with the following primers: forward, 5′-CTG CCT CGG GCG CCA CGG TCT CCC ATG TCT CTG ACA TCG TTG-3′ and reverse, 5′-CAA CGA TGT CAG AGA CAT GGG AGA CCG TGG CGC CCG AGG CAG-3′. pCAG-IP full-length FBL was used as template. PCR products were treated with *Dpn*I at 37°C for 1 h to selectively digest the template plas-

mid. Competent *Escherichia coli* (DH5α) were transformed with *Dpn*I-digested DNA, and the mutated plasmid was selected in LB broth supplemented with ampicillin.

Retroviral vectors, pMXs-Oct4, pMXs-Sox2, pMXs-Klf4, and pMXs-cMyc, were obtained from Addgene (Cambridge, MA). The FBL expression retroviral vector was constructed using a PCR-amplified DNA fragment. The PCR primer set was as follows: forward, 5′-GGA ATT CGC CAC CAT GGA CTA CAA GGA C-3′ and reverse 5′-CTC GCG GCC GCT CAG TTC TTC ACC TTG GGG GG-3′. FBL cDNA was amplified with KOD-Plus, digested with *EcoR*I and *Not*I, and inserted between the *EcoR*I and *Not*I sites of the pMYs vector [15].

Engineered miRNA expression vectors were constructed using the BLOCK-it Pol II miR RNAi expression vector kit (Life Technologies) by inserting the following sense-loop-antisense DNA sequences into the cloning sites of the pcDNA6.2-GW/EmGFP-miR and pcDNA6.2-GW/miR vectors (Life Technologies). The sequences were as follows: FBL miRNA #1, sense, 5′-TGC TGA AAT CAC AAA GTG TCC TCC ATG TTT TGG CCA CTG ACT GAC ATG GAG GAC TTT GTG ATT T-3′, antisense, 5′-CCT GAA ATC ACA AAG TCC TCC ATG TCA GTC AGT GGC CAA AAC ATG GAG GAC ACT TTG TGA TTT C-3′, and FBL miRNA #2, sense, 5′-TGC TGA TTC TTC CCT GAC TGG TTT CCG TTT TGG CCA CTG ACT GAC GGA AAC CAC AGG GAA GAA T-3′, antisense, 5′-CCT GAT TCT TCC CTG TGG TTT CCG TCA GTC AGT GGC CAA AAC GGA AAC CAG TCA GGG AAG AAT C-3′. As a negative control miRNA expression vector, we used the pcDNA 6.2-GW/EmGFP-miR-neg control plasmid (Life Technologies). The negative control sequence without the 5′ overhang was as follows: 5′- GAA ATG TAC TGC GCG TGG AGA CGT TTT GGC CAC TGA CTG ACG TCT CCA CGC AGT ACA TTT-3′.

For the tetracycline (Tc)-off-regulated miRNA expression, the expression cassettes encoding miRNA were amplified with the pcDNA 6.2-GW/EmGFP-mFBL-miR #1 as the template, digested with *Xho*I and *Not*I, and inserted between the *Xho*I and *Not*I sites of the pPhC vector [18]. The primer set was as follows: forward, 5′-AAA CTC GAG TAG GCG TGT ACG GTG GGA GGC CTA TAT AAG CAG AGC TCG TTT AGT GAA CCG TCA GAT CGC CTG GAG AAT TCG CCA CCC TGG AGG CTT GCT GAA G-3′, reverse, 5′-TTT GCG GCC GCA CAC ACA AAA AAC CAA CAC ACA GAT GTA ATG AAA ATA AAG ATA TTT TAT TGG GCC ATT TGT TCC ATG TGA-3′. For the negative control, pcDNA6.2-GW/miR-neg was used as the template for PCR with the same primers.

Similarly, for the overexpression of FBL, the expression cassette encoding FLAG-FBL was amplified, digested with *Xho*I and *Not*I, and inserted between the *Xho*I and *Not*I sites of the pPhC vector.

Tc-off-regulated FBL-miRNA-expressing ES cell lines and Tc-off-regulated FBL-expressing ES cell lines were established according to the method of Masui et al. [18]. An EB3 cell-derived mouse ES cell line, EBRTcH3, which has a Tc-off cassette in the ROSA26 locus, was co-transfected with the above targeting vector, pPthC-FBL-miR or pPthC-FLAG- FBL, and a Cre recombinase-expressing vector, pCAGGS-Cre, using Lipofectamine 2000 (Life Technologies). The cells were cultured in the presence of 1.5 μg/mL puromycin (Sigma-Aldrich) and 1 μg/mL Tc. The established ES clones were cultured in ES medium in the presence or absence of Tc, and the expression of the exogenous gene was examined by immunoblotting and immunofluorescence assay.

For the construction of miRNA-insensitive FBL expression vectors, mutations were introduced into the pCAG-IP-FBL expression vector by PCR-based site-directed mutagenesis using KOD-Plus with the following primers: forward, 5′-CCT GCG TAA TGG TGG ACA TTT CGT AAT ATC CAT TAA GGC CAA CTG-3′ and reverse, 5′-CAG TTG GCC TTA ATG GAT ATT ACG AAA TGT CCA CCA TTA CGC AGG-3′. PCR products were treated with *Dpn*I at 37°C for 1 h to digest selectively the template plasmid, as described above.

Alkaline phosphatase staining

Mouse ES cells were cultured for 10 days in the presence or absence of LIF, fixed with 3.7% formaldehyde in phosphate-buffered saline (PBS) for 5 min at room temperature, and then incubated with an alkaline phosphatase substrate, NBT/BCIP (Roche), at room temperature to visualize the enzyme activity.

Western blotting

Cells were lysed in lysis buffer (20 mM Tris-HCl [pH 7.4], 150 mM NaCl, 1 mM EDTA, 1% Nonidet P-40, 1 mM Na_3VO_4, 25 mM NaF, and 25 mM β-glycerophosphate), supplemented with a protein inhibitor cocktail (Complete, Roche), and rotated at 4°C for 1 h. After centrifugation at 17,000 *g* for 10 min at 4°C, the supernatants were collected and protein concentrations were determined with a protein assay kit (Bio-Rad). Then, 10 μg protein of the whole cell lysate samples were resolved by sodium dodecyl sulfate-polyacrylamide gel electrophoresis and transferred to polyvinylidene fluoride membranes. The membranes were blocked with 5% non-fat skim milk in TBS/Tween-20 (10 mM Tris-HCl [pH 7.4], 150 mM NaCl, 0.1% Tween-20), and incubated with primary antibody overnight at 4°C. After incubation with a horseradish peroxidase-conjugated secondary antibody, the blots were incubated with an enhanced chemiluminescent assay reagent (SuperSignal West Femto, Pierce) for 5 min at room temperature, and the protein bands were visualized using an LAS 1000 Pro Image Analyzer (Fuji Film). For the quantitative analysis, the protein bands were further analyzed using the Image Gauge software (Fuji Film).

Immunofluorescence staining

Mouse ES cells were washed with PBS, fixed in 3.7% formaldehyde in PBS for 30 min at room temperature, and then permeabilized with 0.5% Triton X-100 in PBS

for 5 min at room temperature. The cells were blocked with 5% FCS in PBS for 1 h at room temperature, and then incubated with primary antibodies. After washing 3 times with 5% FCS in PBS for 10 min, the cells were incubated with fluorescently labeled secondary antibodies for 1 h at room temperature, and cell nuclei were stained with 4′,6-diamidino-2-phenylindole (Vector Laboratories). The cells were observed under a fluorescence microscope (Olympus, IX70) equipped with a CoolSNAP HQ^2 (Photometrics) and processed using MetaMorph software (Molecular Devices). A confocal fluorescence microscope (Olympus, FV1000) was also used to analyze the cells.

Immunoprecipitation

Tc-off-regulated FBL-miRNA-expressing ES cells were cultured with or without Tc for 2 days, and subsequently harvested for immunoprecipitation. After preparation of whole cell lysates (1 mg of protein) with the lysis buffer as described above, endogenous Mdm2 was immunoprecipitated with 5 μg of antibody against Mdm2 (Santa Cruz, sc-965) and Dynabeads protein G (Life Technologies, 1004D). The immunoprecipitated proteins were detected by immunoblotting with an antibody against L11 (Santa Cruz, sc-25931). An antibody against α-tubulin (Sigma-Aldrich, T9026, 1:3000) was used as loading control.

Statistical analysis

Values are expressed as the average ± standard errors. The unpaired Student's *t*-test was used for comparisons of the parameters between 2 groups. *p*-values less than 0.05 were considered statistically significant.

RESULTS

FBL is highly expressed in ES cells and promotes pluripotency

Our previous differential proteomic analysis identified FBL, a critical methyltransferase indispensable for rRNA processing, as one of the highly expressed nucleolar proteins in pluripotent ES cells [14]. When mouse ES cells were cultured without leukemia inhibitory factor (LIF) for 10 days, they differentiated into alkaline phosphatase-negative and morphologically flat cells (Figure 1A). Under these conditions, the amount of FBL transcript and protein were significantly decreased, i.e., to about one-third of that found in pluripotent ES cells, as was observed in pluripotency-specific transcription factors, Nanog and Oct4 (Figure 1B-1D). Immunofluorescence analysis further confirmed a decrease in FBL in those cells (Figure 1E). Interestingly, FBL was localized in 1 or 2 large condensed foci in the nuclei in pluripotent ES cells. In contrast, in the differentiated cells and non ES cells FBL was detected in multiple scattered small foci in the nuclei (Figure 1F). A similar morphological change in the nucleoli between pluripotent and differentiated cells has been observed in human ES cells [4]. These results suggested the existence of specific nucleolar functions in pluripotent stem cells.

To explore the functions of nucleoli in ES cells, mouse ES cells stably expressing Flag-tagged FBL were established. These cells showed prolonged alkaline phosphatase activities when cultured without LIF (Figure 2A). FBL-expressing cells showed sustained expression of Oct4, Nanog, and SSEA-1 even when the cells were cultured for 10 days without LIF (Figure 2B, 2C). Furthermore, the morphology of the nucleoli was maintained as large foci in FBL-stably expressing cells (Figure S1). These results suggest that nucleolar FBL has the ability to prolong the pluripotent state of mouse ES cells. In contrast, we did not see a clear effect of exogenous FBL expression on pluripotent ES cells, such as the morphology of ES cells (Figure 2A), the size of nucleoli (Figure S1), and the expression of *Nanog* and *Oct4* (Figure 2B, S2). One possible explanation for this apparent lack of an effect is that the overexpression of FBL on top of the high levels of endogenous FBL in pluripotent stem cells might not produce an effect as robust as the one observed in the differentiated cells.

Next, we examined the effect of FBL on the reprogramming of somatic cells into induced pluripotent stem (iPS) cells [19]. Mouse embryonic fibroblasts (MEFs) were infected with retroviruses that express Oct4, Sox2, Klf4, and c-Myc with or without FBL. Introduction of FBL increased the number of alkaline phosphatase activity-positive colonies as well as the size of the colonies with the transcription factors Oct4, Sox2, and Klf4 (Figure 2D, 2E), suggesting that nucleolar FBL also regulates the reprogramming process of fibroblasts to pluripotent stem cells. However, this effect was not observed with four factors including c-Myc (Figure 2E). *FBL* is one of the downstream target genes of c-Myc [20]. Although overexpression of c-Myc induced *FBL* in MEFs, overexpression of FBL failed to induce *c-Myc* (Figure S3C, S3D). These results suggest that MEFs overexpressing c-Myc already expressed higher levels of endogenous FBL and thus appeared to fail to further promote reprogramming by exogenous FBL.

FBL protein contains a glycine- and arginine-rich (GAR) domain at the N-terminus (Figure S4A). The C-terminal half, containing a central RNA-binding domain (RBD) and α-helical domain, functions as a methyltransferase; it is highly conserved among many FBL orthologs, from archaebacteria to mammals [11]. The N-terminal GAR-domain is only present in eukaryotes [11, 28]. To locate the functional domain of FBL associated with the maintenance of pluripotency, we established mouse ES cells stably expressing Flag-tagged deletion mutants of FBL (FBL-N and FBL-C, Figure S4A). Only ES cells expressing FBL-C showed prolonged alkaline phosphatase activities in the absence of LIF (Figure S4B). Thr-70 of an archaeal FBL has been reported to be an indispensable amino acid for the methyltransferase activity [29]. Stable expression of the corresponding T-to-A mutation at Thr-172 in the human FBL (T172A FBL) in ES cells resulted in flattened mor-

phology and loss of both alkaline phosphatase activity and Nanog protein expression, even in the presence of LIF (Figure S4C). Decreased Nanog expression was also confirmed by quantitative reverse transcription-polymerase chain reaction (qRT-PCR) analysis (Figure S4D). In addition to *Nanog*, the expression of *Eomes* was down-regulated, whereas the differentiation marker *Fgf5* was slightly up-regulated. These results indicate that nucleolar methyltransferase activity is important for the regulation of pluripotency of ES cells.

Nucleolar FBL is indispensable for the survival of pluripotent ES cells

To verify the functional importance of nucleolar methyltransferase in ES cells, mouse ES cells that express FBL-specific engineered miRNA under the control of the tetracycline (Tc)-off inducible promoter were established by using a Cre recombinase-based knock-in method [18]. Removal of Tc from the culture medium induced knockdown of FBL in ES cells (Figure 3A, 3B). Until 48 h after removal of Tc, no significant morphological change in FBL-knockdown cells was observed when ES cells were cultured in the presence of LIF. However, the growth of FBL-knockdown ES cells was clearly decreased on day 3. Within 7 days, most of the knockdown ES cells had disappeared (Figure 3C, 3D). These observations were specific for FBL, as the control miRNA did not show any significant effect on the cell number (Figure 3D). Similar results were also observed with another miRNA against FBL (Figure S5). Knockdown of FBL significantly induced apoptosis (Figure 3E). The ratio of TUNEL-positive cells increased by more than 8-fold when ES cells were cultured for 2 days without Tc (Figure 3F). A 6-fold increase of caspase-activated cells was detected after knockdown of FBL (Figures 3G, 3H). Interestingly, the knockdown of FBL increased apoptosis in pluripotent ES cells but not in the differentiated cells (Figure 3I) and other non-stem cell lines (Figure 3H). We also asked whether the phenotypes of FBL knockdown can be rescued by activating rRNA processing/biosynthesis. c-Myc is a widely recognized upstream regulator that controls the biosynthesis of rRNA by inducing RNA polymerase I [21-23], and it promotes the expression of FBL [20]. However, overexpression of c-Myc failed to inhibit FBL-knockdown-induced apoptosis (Figure S3E, S3F). Only the ectopic expression of the miRNA-insensitive form of FBL rescued ES cells from apoptosis (Figures S6). These results suggest that highly expressed nucleolar FBL is an indispensable terminal rate-limiting enzyme in rRNA processing and in the survival of pluripotent ES cells.

Nucleolar FBL is a principal regulator of rRNA biosynthesis in pluripotent ES cells

Nop1, an ortholog of FBL in yeast, is essential for pre-rRNA processing, and mutations in Nop1 lead to a reduced production rate of mature rRNAs and accumulation of unspliced precursor molecules [10, 12]. Thus, we examined the ribosomal synthesis in FBL-knockdown mouse ES cells using pulse-chase labeling with [^{3}H]-uridine and [methyl-^{3}H]-methionine. Labeling with [^{3}H]-uridine revealed the loss of the 41S precursor and reduction of the 36S precursor, whereas the 34S/32S precursor accumulated in FBL-knockdown ES cells (Figures 4A, 4B). Although both 28S and 18S mature rRNA were reduced in FBL-knockdown ES cells, much less 18S rRNA was synthesized compared to 28S mature rRNA. A pulse chase labeling experiment with [methyl-^{3}H]-methionine revealed an overall delay in rRNA processing and decreased methylation levels of rRNA in FBL-knockdown ES cells. In control cells, 18S and 28S mature rRNA was first detected immediately after the addition of [methyl-^{3}H]-methionine and at 15 min, whereas those of FBL-knockdown ES cells were barely detected at 30 min or 45 min (Figure 4C). In FBL-knockdown ES cells, the amount of methionine-labeled rRNA was decreased to 35% of that in control cells (Figure 4D). Although FBL is the catalytic center of the methyl-transferase complex for rRNA and is essential for the processing of rRNA, there is a possibility that the altered pre-rRNA processing we observed could be one of the indirect outcomes of the complex apoptosis pathway and not a direct consequence of FBL knockdown. To exclude this possibility, we examined the effect of an apoptosis inhibitor on the processing of pre-rRNA (Figure S7A). At 48 h after the induction of FBL knockdown, a statistically significant induction of TUNEL-positive cells was detected. Z-VAD-FMK, a caspase inhibitor, potently suppressed the apoptosis induced by FBL knockdown. However, significant amounts of an intermediate 45S rRNA were still accumulated after treatment with Z-VAD-FMK (Figure S7B), which suggests that altered pre-rRNA processing does not occur as a consequence of apoptosis.

Reduction of ribosomal biosynthesis in nucleoli induces the activation of p53 in ES cells

To examine systematically the effect of the loss of FBL on ES cells, we performed a DNA microarray analysis to screen for the genes that are up- or down-regulated upon knockdown of FBL. Two days after Tc removal, 1,132 entities were up- and 885 entities were down-regulated compared to the control cells (2-fold change). Up-regulated genes were enriched for developmental gene ontology terms in the biological process category (Figure S8A). In contrast, down-regulated genes displayed no significant gene ontology term. Interestingly, the expression of other nucleolar proteins, such as nucleostemin, nucleophosmin, and nucleolin was not changed after FBL-knockdown (data not shown), suggesting that the effects of FBL-knockdown are not the indirect effects caused by the other nucleolar regulators. Bioinformatic pathway analysis identified p53 signaling (p = 2.83E-05) as the most probable pathway specifically activated in FBL-knockdown ES cells (Figure 5A). The activity of p53 is regulated by post-translational modification. Phosphorylation of p53 at

Ser18 is correlated with the induction of cell-cycle arrest/apoptosis [24], and phosphorylation at Ser389 is observed upon UV irradiation [25, 26] or during the differentiation initiated by NO [27] and RA [25]. Immunofluorescence analysis confirmed the induction of p53 expression and its activated form (phosphorylated at Ser18 and at Ser389) after knockdown of FBL in ES cells (Figures 5B, 5C). The activation of p53 could be induced through the binding of ribosomal protein L11 with a p53 inhibitor, Mdm2 [30, 31]. A previous report suggested that upon induction of ribosomal stress, L11 is released from nucleoli into the nucleoplasm, where it associates with Mdm2; this, in turn, rescues p53 from the Mdm2-dependent p53 degradation pathway [31]. Our co-immunoprecipitation experiments also confirmed enhanced binding of Mdm2 with L11 in FBL-knockdown ES cells (Figure. 5D). These results indicate that impaired nucleolar activity by decreasing the rRNA production specifically induces the activation of p53 in ES cells.

Reduction of ribosomal biogenesis also induces the differentiation of ES cells

Whereas complete knockdown of FBL led to apoptosis in ES cells (Figures 3), partial knockdown of FBL promoted their differentiation. In ES cells cultured with 5 ng/mL Tc for 6 days, the FBL protein level decreased to one third of that measured under control conditions (Figures 6A-C), which is similar to the level determined in differentiated cells cultured without LIF (Figure 1B-1D). These cells showed a morphological transition of nucleoli, i.e., from large condensed to small scattered foci, and flattened morphology, even in the presence of LIF (Figures 6A, 6B). qRT-PCR analysis revealed a 5-fold increase in the primitive ectodermal marker *Fgf5* and a more than 2-fold increase in the mesodermal markers *Flk1* and *Brachyury* (*T*). In contrast, pluripotent markers were not affected except for *Oct4* and *Rex1*, which were slightly up-regulated (Figure 6D). In addition, the neural progenitor markers *Pax6* and *Nestin* were up-regulated by about 2-fold compared to the controls (Figure 6D). Immunofluorescence staining also confirmed the up-regulation of these differentiation-specific markers (Figure S9). Similar results were also observed with actinomycin D treatment, which blocks rRNA transcription by inhibiting RNA polymerase I (Figure 6E). Under FBL-reduced culture conditions, p53 and its phosphorylated forms were transiently activated at around day 2 to day 3 of culture (Figures S10). As shown in Figure 6F-G, FBL-knockdown-dependent induction of the early differentiation markers *T* and *Fgf5* was strongly inhibited by the p53-specific inhibitor pifithrin-α (PFTα), which indicates that the FBL-p53 axis controls the differentiation of ES cells. The activation of p53 was also observed during spontaneous differentiation of ES cells cultured in the absence of LIF. Stable expression of FBL inhibited p53 activation and differentiation (Figure S11). One of the kinases responsible for the phosphorylation of p53 at Ser389 is casein kinase II (CK II) [32]. Interestingly, the expression of CK II was induced concomitantly with S389 phosphorylation of p53 (Figure S11A). We further examined the specificity of p53 phosphorylation by CK II with a CK II-specific kinase inhibitor, 5,6-dichloro-1-beta-D-ribofuranosylbenzimidazole. However, this inhibitor did not show a clear inhibition of p53 phosphorylation (data not shown), suggesting the existence of other kinases that can phosphorylate p53 in ES cells.

Next, we asked whether the activity of rRNA production in nucleoli could regulate neuronal differentiation of ES cells. Using Tc-off miRNA FBL knock-in ES cells, monolayer neural differentiation was performed according to a previously published report [33]. After 7 days of culture with 5 ng/mL Tc, the differentiation of $Tuj1^+$ neural cells was enhanced (9.0 ± 1.5%) compared to those cultured under control conditions (1000 ng/mL Tc) (3.1 ± 0.5%) (Figure 7A). Embryoid body-based differentiation also revealed a similar increase in neural differentiation in FBL-partial knockdown cells (Figure 7B). The numbers of both $Tuj1^+$ and $NF200^+$ cells were increased as the Tc concentration decreased (Figures 7C, D). In contrast, overexpression of FBL showed a rather inhibitory effect on this differentiation (Figure 7E, 7F). Tc-off-induced FBL knockdown-dependent differentiation was completely inhibited by PFTα, but not by the caspase-specific inhibitors Z-VAD-FMK and Z-VDVAD-FMK (Figure 7G, 7H), indicating that a reduction in FBL levels induces the differentiation of ES cells in a p53-dependent manner, which is independent from apoptosis-dependent activation of p53. These results demonstrate that the decrease in rRNA production can control the efficiency of ES cell differentiation.

DISCUSSION

Nucleoli are the centers of rRNA biosynthesis, and their size reflects ribosomal activity, cell-cycle progression, and proliferation [6, 34]. Hypertrophy of the nucleoli has been reported as one of the most distinctive cytological features of cancer cells [35]. In contrast, defects in ribosomal activity are associated with several inherited bone marrow failure syndromes, e.g., Diamond-Blackfan, and characterized by a decreased number of erythroid progenitors as well as a variety of abnormalities during development, e.g., congenital and growth retardation [36, 37].

In ES cells, large and condensed nucleoli are one of the hallmarks of pluripotency [4]. The morphology of the nucleoli changes from large to scattered, small foci during the differentiation of ES cells. In this study, we have shown that ES cells stably expressing FBL, a critical regulator of rRNA synthesis, retained pluripotency-state-specific large nucleoli for a longer time in the absence of LIF and prolonged their pluripotency. In contrast, when the status of nucleoli was changed to the differentiated state by reducing the expression of FBL to the level of differentiated cells, the ES cells became partially differentiated even under self-renewing culture conditions. These results clearly indicate that the nucleolar state, i.e., the activity of ribosome biogenesis,

controls the pluripotency of ES cells. We further demonstrated that a decrease in the nucleolar activity by partial knockdown of FBL promotes neural differentiation.

In FBL-knockdown ES cells, complete shutdown of rRNA biosynthesis triggered p53 activation, and induced apoptosis. This could be due to nucleolar stress-dependent activation of p53 signaling followed by cell-cycle arrest in ES cells [30, 31]. On the other hand, modulation of the nucleolar activity to a level similar to that of the differentiated state by reducing FBL expression could mildly activate p53 and induce the differentiation of ES cells even in the presence of LIF. The differentiation of ES cells induced by the modification of rRNA biosynthesis was completely suppressed by a p53 inhibitor, PFTα. Therefore, the activity of rRNA biosynthesis could control not only apoptosis but also differentiation of ES cells via the p53 signaling pathway.

Several proteins localized in the nucleolus have been suggested to regulate ES cells proliferation and survival. Nucleostemin was shown to participate in controlling cell proliferation and survival in ES cells [38, 39]. In addition, nucleophosmin 1 is essential for mouse ES cell growth [40, 41]. However, these two proteins do not directly regulate biosynthesis of rRNA, and the curious relationship between unique nucleolar morphology i.e. regulation of ribosomal biogenesis and the ES cell-specific characteristics, i.e. pluripotency and differentiation, has not been elucidated.

In this study, we demonstrated that biosynthesis of rRNA itself could regulate pluripotency of ES cells by modulating a principal protein for ribosome biogenesis, FBL, and also showed that inhibition of rRNA transcription triggers the expression of differentiation-associated markers by an RNA polymerase I-specific inhibitor, actinomycin D. Our results suggest that rRNA biosynthesis in the nucleolus is a novel regulator for not only pluripotency but also preventing ES cells from differentiating. Very recently, involvement of rRNA transcription in the proliferation and cell fate decision has also been reported in the other stem cells, ovarian germ line stem cells in *Drosophila* [42] and mouse hematopoietic stem cells [43].

For several decades, researchers have been describing the relationship between nucleolar size, rRNA biosynthesis, cell proliferation, and development. Down-regulation of nucleolar activity during differentiation has been reported in various tissues. For example, reduction of the nucleolar size has been reported during maturation of the intestinal epithelium in rat [44], epidermal maturation in chick [45], and eye differentiation in *Drosophila* [46]. p53 is also expressed in various organs during development, and its expression level is significantly down-regulated as differentiation proceeds [47, 48]. Although p53-null mice are viable, previous studies suggested the importance of p53 in normal development in several tissues, e.g., the nervous system, eyes, hind limbs, and teeth [49, 50]. However, the regulatory mechanism of p53 remains controversial. Considering these *in vivo* observations, our results raise the hypothesis that down-regulation of the ribosomal activity in nucleoli could trigger the activation of the p53 signaling pathway and induce differentiation of various tissues *in vivo*. Further study is needed to verify the relationship between nucleolar activity and differentiation *in vivo*.

Conclusion

We have identified a novel regulatory function of nucleoli in pluripotent stem cells. We have shown that biosynthesis of rRNA in nucleoli is a unique regulator of pluripotency as well as the differentiation of stem cells. Our study suggests that strict regulation of nucleolar activity together with the transcriptional network control pluripotency and differentiation of ES cells.

Acknowledgement

The plasmid vectors (pPthC and pCAGGS-Cre) and the mouse ES cell line EBRTcH3 were kind gifts from Drs. Niwa and Masui (RIKEN, Japan). The expression vector pCAG-IP was generously given by Dr. Koide (Kanazawa University, Japan). Expression vectors of FBL (pcDNA3.1(+)-FBL and the deletion mutants) were kind gift from Dr. Takahashi (Tokyo University of Agriculture and Technology). Plat-E cells were kindly provided from Dr. Kitamura (University of Tokyo, Japan). KUM9 cells were generously provided from Dr. Umezawa (NCCHD, Japan) via JCRB cell bank (Osaka, Japan).

Competing Interests

The authors have declared that no competing interests exist.

Author Contributions

K.W.: Collection and/or assembly of data, Data analysis and interpretation, Manuscript writing, Final approval of manuscript.; H.T.: Collection and/or assembly of data, Data analysis and interpretation, Manuscript writing, Final approval of manuscript.; K.E.: Conception and design, Collection and/or assembly of data, Data analysis and interpretation.; K.M.: Collection and/or assembly of data.; H.I.: Collection and/or assembly of data; A.I.: Collection and/or assembly of data; M.O.: Provision of study material; M.N.: Provision of study material; Hiromu Sugino: Conception and design.; M.A.: Conception and design, Financial support.; A.K.: Conception and design, Financial support, Data analysis and interpretation, Manuscript writing, Final approval of manuscript.

REFERENCES

1 Niwa, H., Ogawa, K., Shimosato, D., *et al.* (2009). A parallel circuit of LIF signalling pathways maintains pluripotency of mouse ES cells. Nature 460, 118-122.

2 Ng, H.H., and Surani, M.A. (2011). The transcriptional and signalling networks of pluripotency. Nat. Cell Biol. 13, 490-496.

3 Meshorer, E., Yellajoshula, D., George, E., *et al.* (2006). Hyperdynamic plasticity of chromatin proteins in pluripotent embryonic stem cells. Dev. Cell 10, 105-116.

4 Meshorer, E., and Misteli, T. (2006). Chromatin in pluripotent embryonic stem cells and differentiation. Nat. Rev. Mol. Cell Biol. 7, 540-546.

5 Hadjiolov, A.A. (1985). The nucleolus and ribosome biogenesis. in: Cell Biology Monographs, Springer-Verlag, New York. pp. 1–263.

6 Boisvert, F.M., van Koningsbruggen, S., Navascués, J., *et al.* (2007). The multifunctional nucleolus. Nat. Rev. Mol. Cell Biol. 8, 574-585.

7 Shaw, P.J. and Jordan, E.G. (1995). The nucleolus. Annu. Rev. Cell Dev. Biol. 11, 93-121.

8 Nakamoto, K., Ito, A., Watabe, K., *et al.* (2001). Increased expression of a nucleolar Nop5/Sik family member in metastatic melanoma cells: evidence for its role in nucleolar sizing and function. Am. J. Pathol. 159, 1363–1374.

9 Mosgoeller, W. (2004). Nucleolar ultrastructure in vertebrates. The Nucleolus (ed. by M. O. J. Olson), pp. 10–20. Kluwer Academic Press, New York, New York.

10 Schimmang, T., Tollervey, D., Kern, H., *et al.* (1989). A yeast nucleolar protein related to mammalian fibrillarin is associated with small nucleolar RNA and is essential for viability, EMBO J. 8, 4015–4024.

11 Aris, J.P., and Blobel, G. (1991). cDNA cloning and sequencing of human fibrillarin, a conserved nucleolar protein recognized by autoimmune antisera. Proc. Natl. Acad. Sci. 88, 931-915.

12 Tollervey, D., Lehtonen, H., Jansen, R., *et al.* (1993). Temperature-sensitive mutations demonstrate roles for yeast fibrillarin in pre-rRNA processing, pre-rRNA methylation, and ribosome assembly. Cell 72, 443-447.

13 Newton, K., Petfalski, E., Tollervey, D., *et al.* (2003). Fibrillarin is essential for early development and required for accumulation of an intron-encoded small nucleolar RNA in the mouse. Mol. Cell. Biol. 23, 8519–8527.

14 Intoh, A., Kurisaki, A., Fukuda, H., *et al.* (2009). Separation with zwitterionic hydrophilic interaction liquid chromatography improves protein identification by matrix-assisted laser desorption/ionization-based proteomic analysis. Biomed. Chromatogr. 23, 607-614.

15 Morita, S., Kojima, T., and Kitamura, T. (2000). Plat-E: an efficient and stable system for transient packaging of retroviruses. Gene Ther. 7, 1063-1066.

16 Yanagida, M., Hayano, T., Yamauchi, Y., *et al.* (2004). Human fibrillarin forms a subcomplex with splicing factor 2-associated p32, protein arginine methyltransferases, and tubulins alpha 3 and beta 1 that is independent of its association with preribosomal ribonucleoprotein complexes. J. Biol. Chem. 279, 1607-1614.

17 Yoshida-Koide, U., Matsuda, T., Saikawa, K., *et al.* (2004). Involvement of Ras in extraembryonic endoderm differentiation of embryonic stem cells. Biochem. Biophys. Res. Commun. 313, 475-481.

18 Masui, S., Shimosato, D., Toyooka, Y., *et al.* (2005). An efficient system to establish multiple embryonic stem cell lines carrying an inducible expression unit. Nuc. Acids Res. 33, e43.

19 Takahashi, K., and Yamanaka, S. (2006). Induction of pluripotent stem cells from mouse embryonic and adult fibroblast cultures by defined factors. Cell. 126, 663-676.

20 Coller H.A., Grandori C., Tamayo P., *et al.* (2000). Expression analysis with oligonucleotide microarrays reveals that MYC regulates genes involved in growth, cell cycle, signaling, and adhesion. Proc. Natl. Acad. Sci. U S A. 97, 3260-3265.

21 Arabi A., Wu S., Ridderstråle K., *et al.*, (2005). c-Myc associates with ribosomal DNA and activates RNA polymerase I transcription. Nat. Cell Biol. 7, 303–310

22 Grandori C, Gomez-Roman N, Felton-Edkins ZA., *et al.*, (2005). c-Myc binds to human ribosomal DNA and stimulates transcription of rRNA genes by RNA polymerase I. Nature Cell Biol. 7, 311–318.

23 Grewal, S.S., Li, L., Orian, A., *et al.*, (2005). Myc-dependent regulation of ribosomal RNA synthesis during Drosophila development. Nat. Cell Biol. 7, 295–302

24 Smeenk L., van Heeringen S.J., Koeppel M. *et al.*, (2011). Role of p53 serine 46 in p53 target gene regulation. PLOS ONE, 6, e17574.

25 Lin T., Chao C., Saito S., *et al.*, (2005). p53 induces differentiation of mouse embryonic stem cells by suppressing Nanog expression. Nat. Cell Biol. 7, 165-171.

26 Kapoor, M., and Lozano, G. (1998). Functional activation of p53 via phosphorylation following DNA damage by UV but not gamma radiation. Proc. Natl. Acad. Sci. USA 95, 2834–2837

27 Mora-Castilla S., Tejedo J.R., Hmadcha A., *et al.*, (2010). Nitric oxide repression of Nanog promotes mouse embryonic stem cell differentiation. Cell Death Differ. 17, 1025-1033.

28 Wang, H., Boisvert, D., Kim, K.K., *et al.* (2000). Crystal structure of a fibrillarin homologue from Methanococcus jannaschii, a hyperthermophile, at 1.6 A resolution. EMBO J. 19, 317–323.

29 Aittaleb, M., Visone, T., Fenley, M.O., *et al.* (2004). Structural and thermodynamic evidence for a stabilizing role of Nop5p in S-adenosyl-L-methionine binding to fibrillarin. J. Biol. Chem. 279, 41822-41829.

30 Morgado-Palacin, L., Llanos, S., and Serrano, M. (2012). Ribosomal stress induces L11- and p53-dependent apoptosis in mouse pluripotent stem cells. Cell Cycle 11, 503-510.

31 Suzuki, A., Kogo, R., Kawahara, K., *et al.* (2012). *A new PICTure of nucleolar stress*. Cancer Sci. 103, 632-627.

32 Meek, D.W., Simon, S., Kikkawa, U., *et al.* (1990). The p53 tumour suppressor protein is phosphorylated at serine 389 by casein kinase II. EMBO J. 9, 3253–3260.

33 Ying, Q.L., Starvridis, M., Griffiths, D., *et al.* (2003). Conversion of embryonic stem cells into neuroectodermal precursors in adherent monoculture. Nat. Biotechnol. 21, 183-186.

34 Derenzini, M., Trerè, D., Pession, A., *et al.* (2000). Nucleolar size indicates the rapidity of cell proliferation in cancer tissues. J. Pathol. 191, 181–186.

35 Montanaro, L., Trere, D., and Derenzini, M. (2008). Nucleolus, ribosomes and cancer. Am. J. Pathol. 173, 301-310.

36 Ganapathi, K.A., and Shimamura, A. (2008). Ribosomal dysfunction and inherited marrow failure. Br. J. Haematol. 141, 376-387.

37 Vlachos, A., Ball, S., Dahl, N., *et al.* (2008). Diagnosing and treating Diamond Blackfan anaemia: results of an international clinical consensus conference. Br. J. Haematol. 142, 859-876.

38 Nomura, J., Maruyama, M., Katano, M., *et al.* (2009). Differential requirement for nucleostemin in embryonic stem cell and neural stem cell viability. Stem Cells. 27, 1066-1076.

39 Qu, J., and Bishop, J.M. (2012). Nucleostemin maintains self-renewal of embryonic stem cells and promotes reprogramming of somatic cells to pluripotency. J. Cell Biol. 197, 731-745.

40 Wang, B.B., Lu, R., Wang, W.C., *et al.* (2006). Inducible and reversible suppression of Npm1 gene expression using stably integrated small interfering RNA vector in mouse embryonic stem cells. Biochem. Biophys. Res. Commun. 347, 1129-1137.

41 Abujarour, R., Efe, J., and Ding, S. (2010). Genome-wide gain-of-function screen identifies novel regulators of pluripotency. Stem Cells. 28, 1487-1497.

42 Zhang Q, Shalaby N.A., Buszczak M. (2014). Changes in rRNA transcription influence proliferation and cell fate within a stem cell lineage. Science 343, 298-301.

43 Hayashi Y., Kuroda T., Kishimoto H., *et al.* (2014). Downregulation of rRNA transcription triggers cell differentiation. PLOS ONE 9, e98586.

44 Altmann, G.G., and Leblond, C.P. (1982). Changes in the size and structure of the nucleolus of columnar cells during their migration from crypt base to villus top in rat jejunum. J. Cell Sci. 56, 83-99.

45 Zavala, G., and Vázquez-Nin, G.H. (1997). Changes of ribonucleoproteic structures of embryonic epidermal cell nuclei during differentiation and maturation. Biol. Cell. 89, 245-255

46 Baker, N.E. (2013). Developmental regulation of nucleolus size during *Drosophila* eye differentiation. PLOS ONE 8, e58266.

47 Rogel, A., Popliker, M., Webb, C.G., *et al.* (1985). p53 cellular tumor antigen: analysis of mRNA levels in normal adult tissues, embryos, and tumors. Mol. Cell. Biol. 5, 2851-2855.

48 Schmid, P., Lorenz, A., Hameister, H., *et al.* (1991). Expression of p53 during mouse embryogenesis. Development. 113, 857-865.

49 Armstrong, J.F., Kaufman, M.H., Harrison, D.J., *et al.* (1995). High-frequency developmental abnormalities in p53-deficient mice. Curr. Biol. 5, 931-936.

50 Sah, V.P., Attardi, L.D., Mulligan, G.J., *et al.* (1995). A subset of p53-deficient embryos exhibit exencephaly. Nat. Genet. 10, 175-180.

See www.StemCells.com for supporting information available online. STEM CELLS; *00:000–000*

Figure 1. FBL is highly expressed in pluripotent ES cells. Mouse ES cells were cultured for 10 days in the presence (+LIF) or absence of LIF (-LIF) and analyzed for pluripotency marker protein expression. (A) Alkaline phosphatase staining. ES cells cultured in the presence of LIF formed tightly packed colonies and had high alkaline phosphatase activity (upper panel), whereas ES cells cultured in the absence of LIF for 10 days showed flattened morphology and lower alkaline phosphatase activity (lower panel). (B) qRT-PCR analysis of *FBL* mRNA. The ES cells were cultured as in (A) for 10 days. (C) Western blot analysis of FBL, Nanog, and Oct4 expression. (D) Relative densitometric values of the bands. Values were normalized to α-tubulin. Expression levels of FBL, Nanog, and Oct4 in (C) cultured without LIF for 10 days were approximately 36%, 24%, and 30% of that of the cells cultured with LIF, respectively. (E) Immunofluorescence staining of FBL, Nanog, Oct4, and SSEA-1. The ES cells were cultured as in (A) for 10 days. (F) Localization of FBL in pluripotent and differentiated cells. Arrowheads indicate immunoreactivity of FBL in the nucleus. *$p < 0.01$ in (B, D). Scale bars: (A), 300 μm; (E), 30 μm; (F), 20 μm.

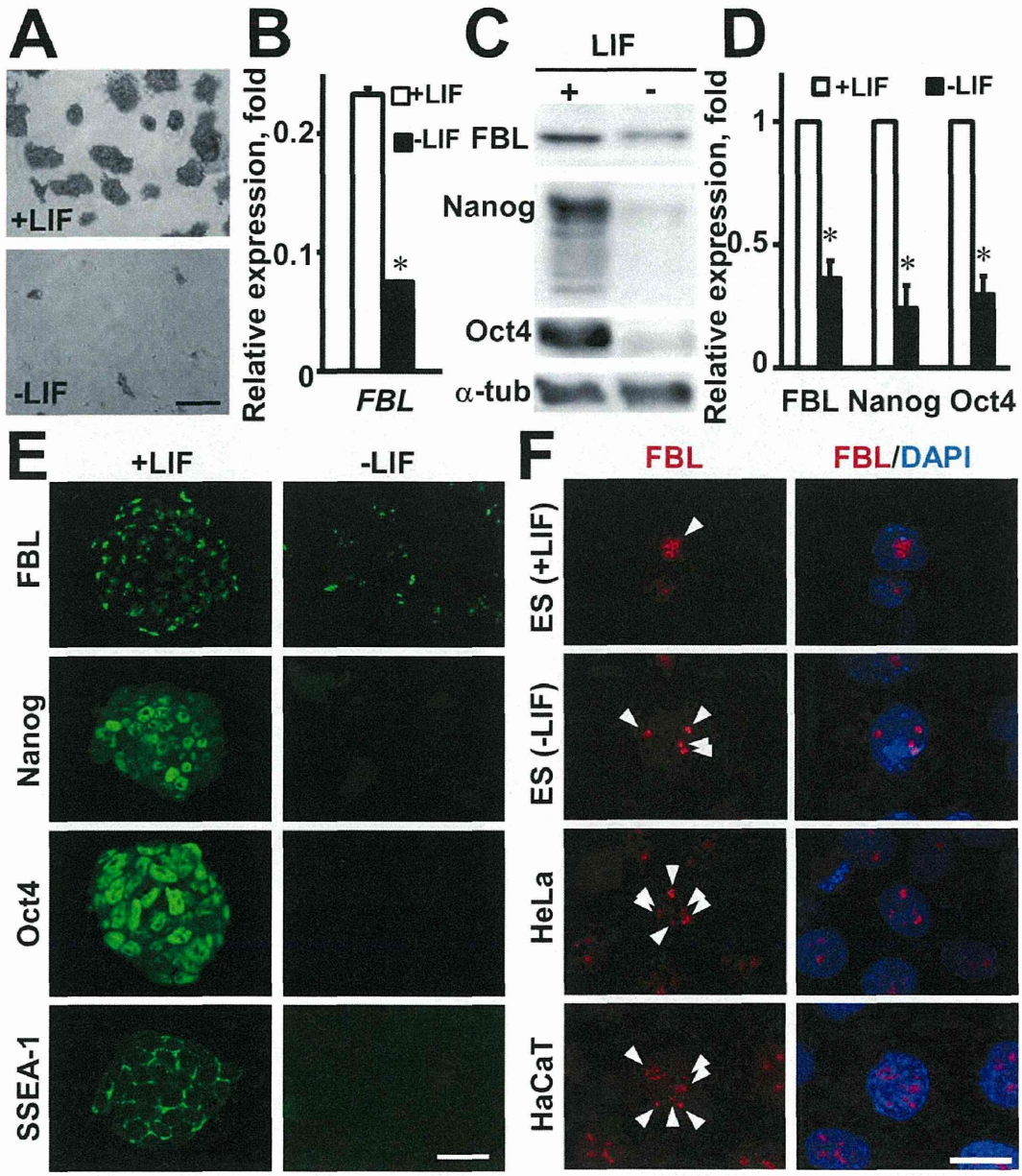

Figure 2. Stable expression of FBL prolongs the pluripotency of ES cells in the absence of LIF. ES cells stably expressing FBL or the control vector were cultured for 10 days in the presence or absence of LIF, and the expression levels of pluripotency-specific markers were analyzed. (A) Alkaline phosphatase staining of ES cells stably expressing FBL. (B) Western blot analysis of Nanog, Oct4, FBL, and FLAG antibodies. (C) Immunofluorescence analysis of ES cells with Nanog, Oct4, and SSEA-1 antibodies after culturing without LIF for 10 days. (D, E) FBL enhances reprogramming efficiency of MEFs. (D) Alkaline phosphatase staining of iPS cells induced with retroviruses for 4 transcription factors (Oct4, Sox2, Klf4, and cMyc) or 3 transcription factors (Oct4, Sox2, and Klf4) with or without FBL expression virus. Empty vector pMYs virus was used as control. (E) The colony numbers of iPS cells were counted and normalized to that of the control. Induction of iPS cells was assayed three times independently. Scale bars: (A), 200 μm; (C), 30 μm.

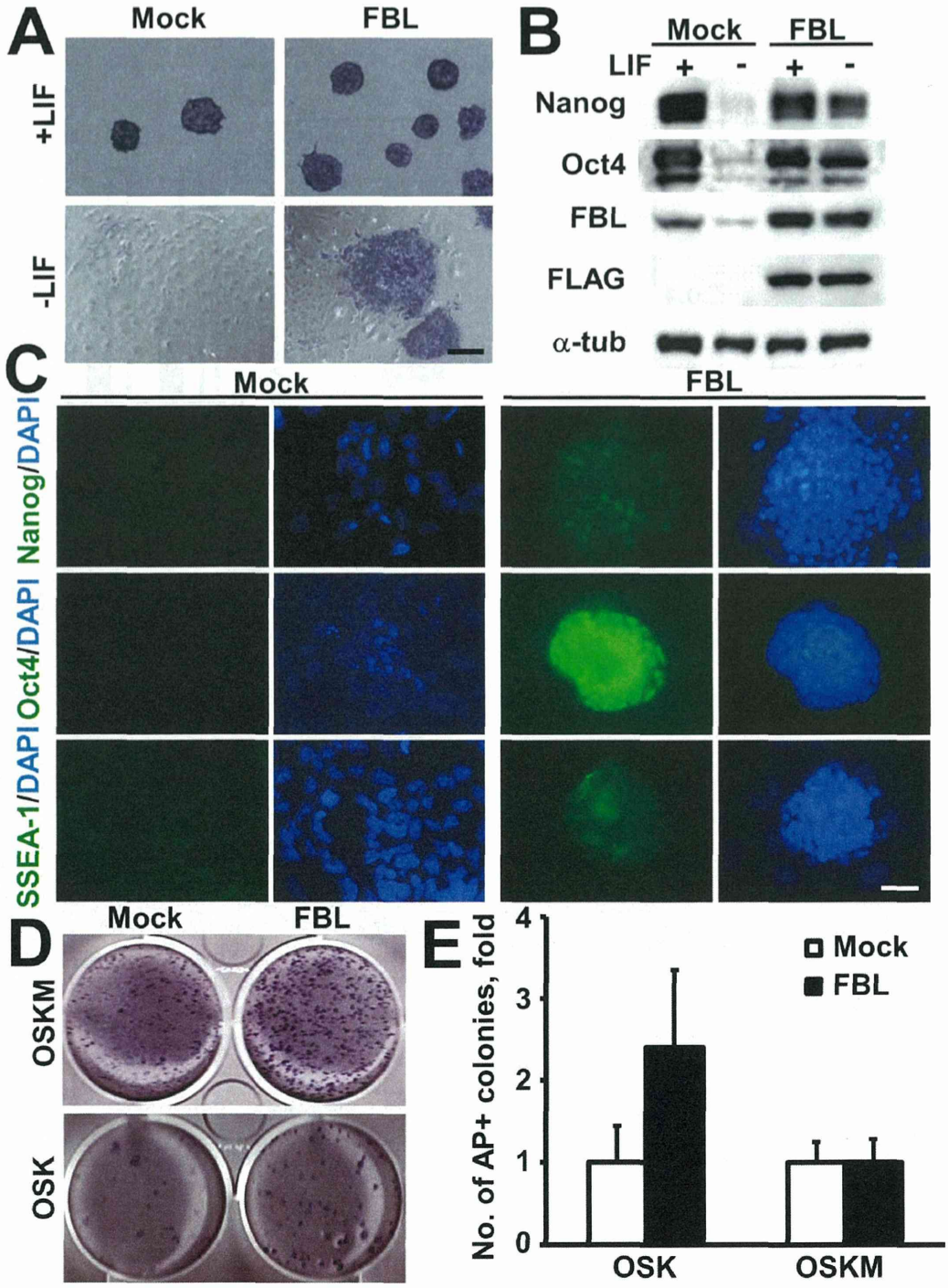

Figure 3. FBL is indispensable for the survival of ES cells. Tc-inducible FBL miRNA-expressing mouse ES cell lines were established and analyzed. (A) Immunofluorescence analysis of FBL expression. Upon withdrawal of Tc, FBL expression was notably decreased (middle and right). Cells were immunostained after 2 days of culture in the absence of Tc. (B) Western blot analysis of FBL expression in (A). A control miRNA did not affect the expression of FBL. (C) Morphological changes in FBL-knockdown ES cells under feeder-free culture conditions. After induction of FBL miRNA (-Tc), colonies of ES cells decreased in size and number at day 3, and had gradually disappeared by day 7. (D) Quantification of (C) by counting cell numbers after 3 days of culture. The data for control miRNA was shown on the left. (E) Significant increase in the number of TUNEL- or activated caspase-positive cells among FBL-knockdown ES cells cultured for 2 days in the absence of Tc. (F) Quantification of TUNEL-positive cells in (E). (G) Activated caspase staining of ES cells. GFP expression indicates the transfected cells with either GFP-control miRNA or GFP-FBL miRNA expression vector. (H) Apoptotic cell death caused by FBL-knockdown was significant in ES cells but not in other cell lines. Quantification of activated caspase-positive cells was performed 2 days after transfection with GFP-control miRNA or GFP-FBL miRNA expression vector. (I) Quantification of caspase-positive cells in ES cells. In the presence of LIF, ES cells were cultured with or without Tc for 2 days. In the absence of LIF, ES cells were pre-cultured in the presence of Tc for 7 days, further cultured with or without Tc for 2 days, and percentage of caspase-positive cells were analyzed. $*p < 0.01$ in (D, F, and H). $*p < 0.05$ in (I). Scale bars: (A), 30 μm; (C), 300 μm; (E, G), 50 μm.

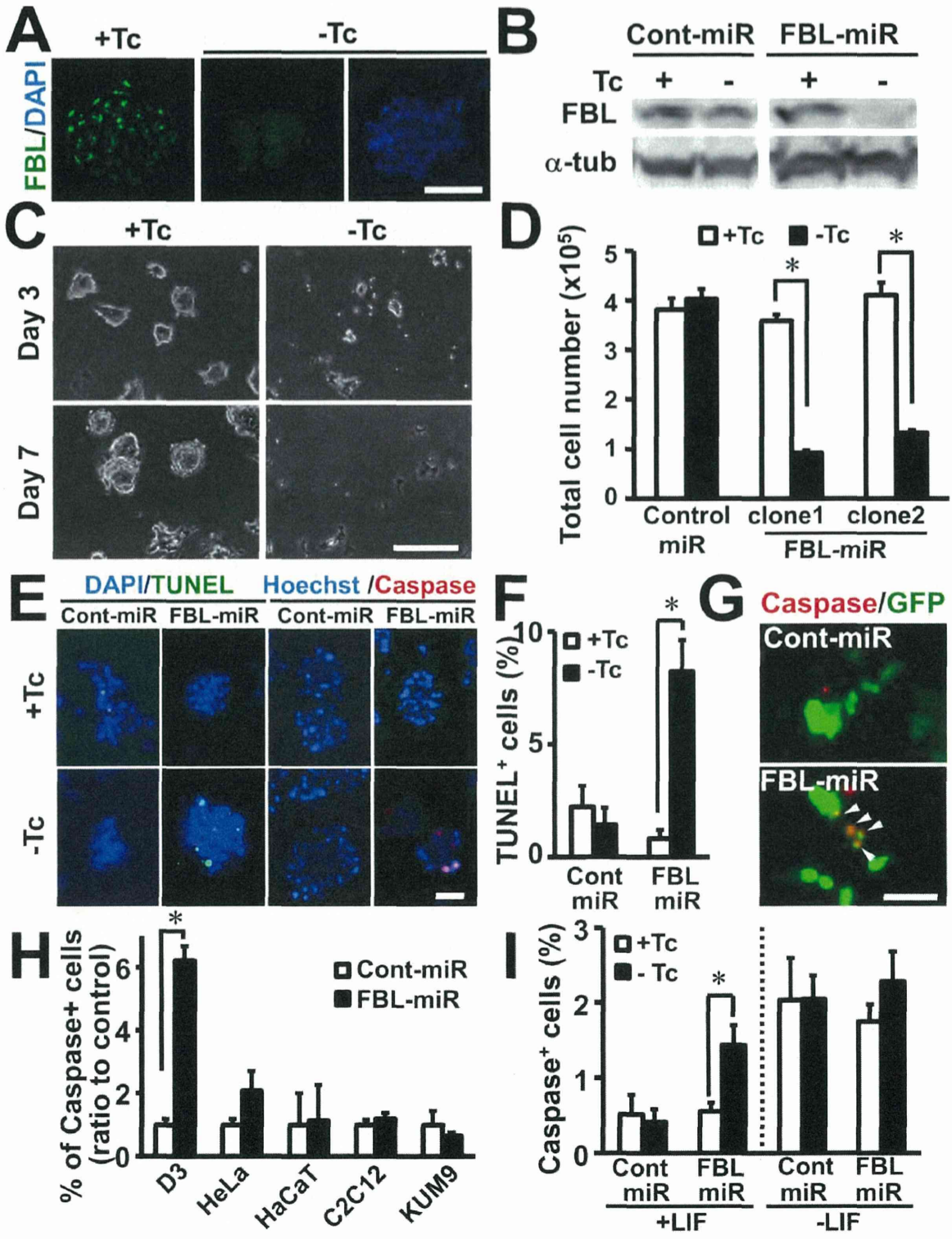

Figure 4. Knockdown of FBL in ES cells disturbs normal processing of pre-rRNA. (A, B) Pulse-chase labeling of ES cells with [^{3}H]-uridine. The ES cells were cultured with or without Tc for 2 days before labeling. (A) Autoradiography of total RNAs. The levels of 41S and 36S intermediate products and mature rRNA, 28S and 18S, were decreased in FBL-knockdown ES cells (-Tc). (B) Quantification of rRNA processing products. Each band was measured and divided by the sum of all products. Intermediate products, 47S/45S pre-rRNA and 34S/32S, were accumulated under FBL-knockdown conditions compared to control conditions. In contrast, the levels of mature forms of rRNA, 18S and 28S, were decreased under FBL-knockdown conditions. (C, D) Pulse-chase labeling with [methyl-^{3}H]-methionine. (C) Autoradiography of total RNAs. As in the case of [^{3}H]-uridine labeling, the levels of 41S and 36S intermediate products were decreased under FBL-knockdown conditions. (D) Quantification of methylated rRNA products. Graph shows the comparison of relative densitometric values of methylated rRNA products. Each experiment was performed two times and the data were averaged.

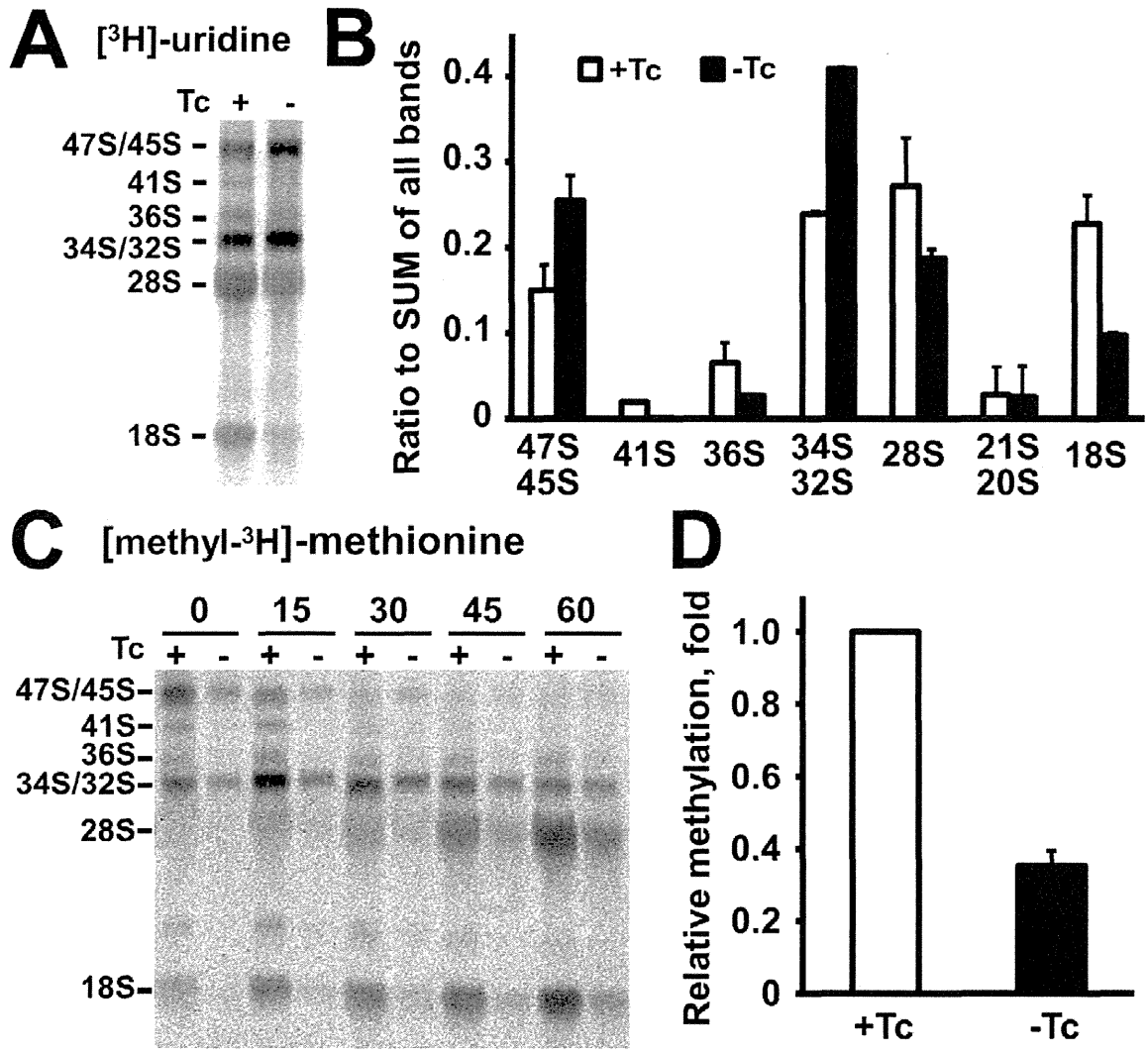

Figure 5. p53 signaling was specifically activated in FBL-knockdown ES cells. (A) Pathway analysis of microarray data obtained with FBL-knockdown ES cells. ES cells were cultured in the absence of Tc for 2 days. p53 signaling was identified as the most activated canonical pathway after knockdown of FBL. (B) Immunofluorescence analysis of p53 and p53 phosphorylation at Ser18 and Ser389 in FBL-knockdown ES cells cultured in the absence of Tc for 2 days. (C) Western blot analysis of p53 protein in ES cells cultured for 2 days without Tc. The lower graph shows the comparison of relative densitometric values of the bands. Values were normalized to Gapdh. Expression levels of p53 were 7.8-fold up-regulated in the absence of Tc (FBL-knockdown conditions). (D) Co-immunoprecipitation analysis of L11 and Mdm2 interaction using ES cells cultured for 2 days after knockdown of FBL. Scale bar: (B), 20 μm. *$p < 0.01$ in (C).

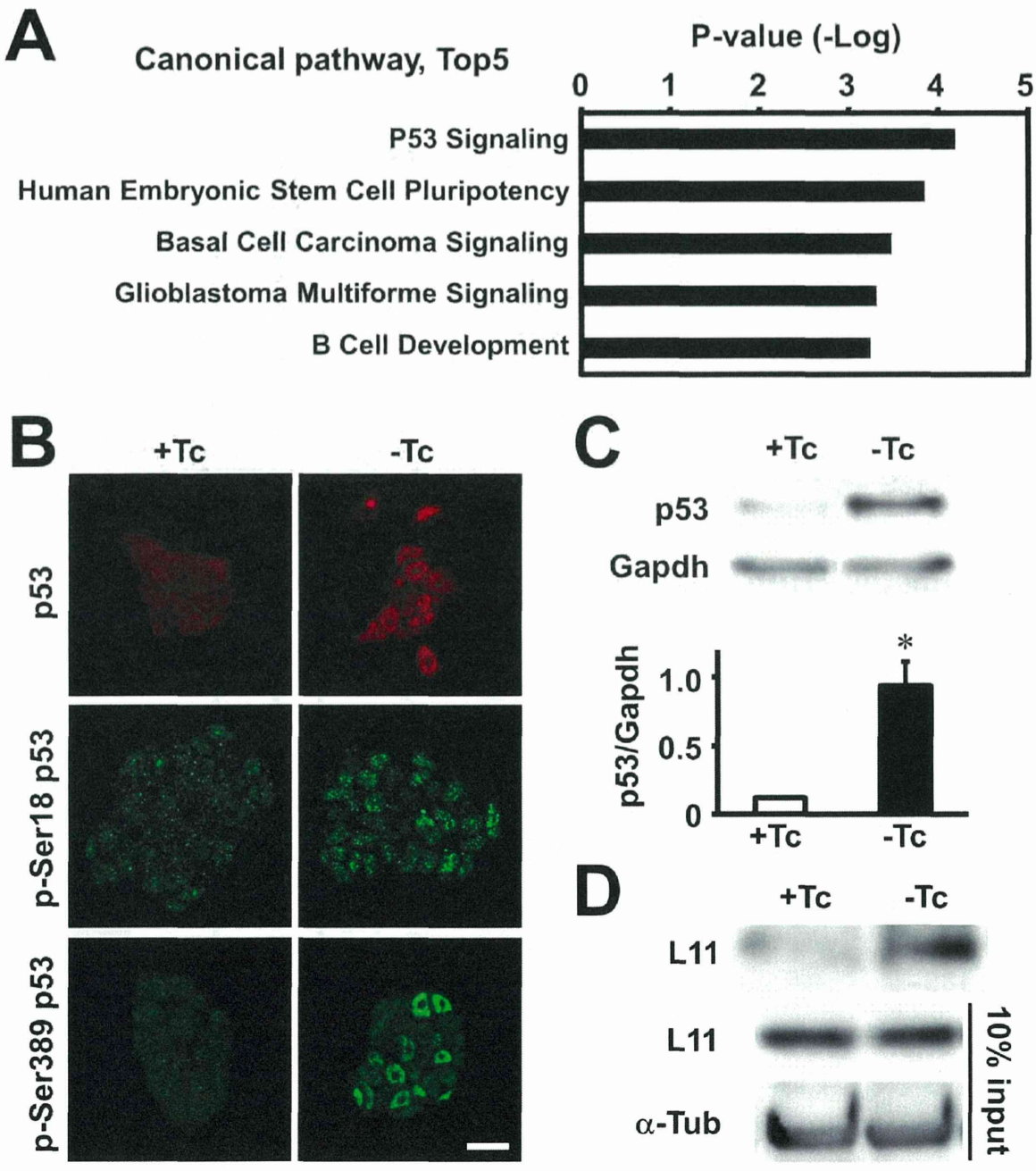

Figure 6. Reduction of FBL expression induces differentiation marker expression via the p53 signaling pathway under self-renewal culture conditions. (A) ES cells cultured for 6 days with 5 ng/mL of Tc resulted in the loss of the densely packed morphology. (B) Immunofluorescence analysis of FBL in (A). (C) Western blot analysis of ES cell extracts after partial knockdown of FBL. FBL expression was decreased to about one-third of that of control conditions after 6 days of culture with 5 ng/mL Tc. (D) qRT-PCR analysis of differentiation- and pluripotency-specific marker expression for each culture condition. After 6 days of culture, the expression of differentiation markers increased, whereas the expression of pluripotency markers was not changed under FBL-reduced conditions. (E) qRT-PCR analysis of differentiation- and pluripotency-specific marker expression 24h after administration of 4 ng/mL actinomycin-D (ActD). (F) Morphological changes in ES cells. ES cells were cultured under self-renewal conditions, and pifithrin-α (PFTα) or DMSO was added from the beginning of culture. In the presence of PFTα, colonies retained their densely packed morphology, even after partial knockdown of FBL. (G) qRT-PCR analysis of the expression of differentiation markers. PFTα treatment suppressed the expression of differentiation markers, *T* and *Fgf5*, in a dose-dependent manner. $*p < 0.01$ in (C, E, and G). $*p < 0.05$ in (D). Scale bars: (A) 300 μm; (B) 10 μm; (F) 500 μm.